The Eurasia Proceedings of Science, Technology, Engineering & Mathematics (EPSTEM)
ISSN: 2602-3199

The Eurasia Proceedings of Science, Technology, Engineering & Mathematics (EPSTEM), 2023

Volume 25, Pages 187-195

ICBAST 2023: International Conference on Basic Sciences and Technology

Thermal Oxidation Kinetics of Nickel and Dilute (Ni-Al) Alloys

Nacer Halem
University Mouloud Mammeri

Zohra Halem
University of Bouira

Petot-Ervas Georgette
Centrale Supelec

Abstract: Oxidation of high purity nickel and of a dilute Ni-Al (0.11 wt%) polycrystalline alloy were performed in the temperature range 700 - 1200°C, under P_{O2}=1 atm. At T<1100°C, Al leads to a reduction of the oxidation kinetic, while at higher temperatures its beneficial effect disappears. The results were analysed from a formal treatment, taking into account the thermodynamic and transport properties of undoped and Al-doped $Ni_{1-x}O$ single crystals. At temperatures below 1000°C, it was found that the results are in agreement with the thermal oxidation of undoped and doped $Ni_{1-x}O$ samples. They are due to the kinetic demixing of cations in the alloy layer growth, leading to both, a lower concentration of aluminium and a decrease of D_{Ni} in the outer oxidation scale. At higher temperatures, the Ni-Al alloy oxidises faster than Ni. This increase was explained by an inward oxygen gas transport within the layer through fissures, whose formation was attributed to compressive stresses due to the growth of nickel oxide units in grain boundaries. The mechanism whereby nickel oxide units form is explained.

Keywords: Oxidation rate, Kinetic demixing, Thermodynamic, Diffusion, Point defects.

Introduction

When metals or alloys are used in high–temperature oxidizing environments, an oxide scale can develop at their surface (Stott,1977; Wood, 1966; Wagner, 1951; Kofstad ,1988, 2007; Atkinson, 1983; Schmalzried, 1981; Catlow,1986). This layer can then act as a protection barrier, to continuing attack by the surrounding atmosphere. The requirement for an effective protection of this barrier imposes a low diffusion of the reactants and the absence of pores and cracks in the oxide scale. However, present understanding of oxidation mechanisms concerned is poor because oxidation results were analysed generally from observatios done at room temperature, influenced by transport processes occurring during cooling (Petot-Ervas, 1990; Halem, 2016). The purpose of this work was to explain oxidation rates from a general treatment of transport processes in p-type semiconducting oxides under non-equilibrium conditions, using the transport properties of mobile species. A Ni-Al alloy was chosen because both, the ionic size of Al^{3+} allows that it should replace substitutionnally Ni^{2+} and its valence state is independent of T and P_{O2}.

Method

Statement of the problem

The thermal oxidation of nickel is considered as a model system for oxidation studies of metals because of its apparent simplicity. Indeed, NiO is the only oxide stable at high temperature and the oxidation rate is controlled by the outward diffusion of Ni^{2+} through the scale, according to a parabolic law. However almost all studies were done from observations at room temperature, as indicated in the introduction. Such analyses leaves much to be desired, since authors don't provide a rationalization for the presence of precipitates, for instance, altough they use them in their analyses.

General Equations in P-Type Semiconducting Oxides at the Thermodynamical Equilibrium

If one considers a cation deficient p-type semiconducting solid solution (AO-BO□), such as $Al_2O_□$ doped $Ni_{1-x}O$, the prevailing defects are electron holes (h°) and □ time ionized cationic vacancies ($V^{□'}$). The defects are introduced by reaction with the surrounding atmosphere ($½O_2 <=> O_O + V^{□'} + □h^{\circ}$). Their concentration depends on temperature (T) and oxygen partial pressure (P_{O2}) in equilibrium with the sample (Philibert,1991), (Atkinson , 1981), (Farhi, 1978).

$$[h^{\circ}] = □[V^{□'}] = AK_V^{1/(□+1)} (P_{O2})^{1/2(□+1)} \quad (1)$$

where K_V is the equilibrium constant of formation of the defects, O_O an oxygen ion on its normal lattice site, $A=□^{1/(□+1)}$ and the square brackets (or x_i) indicate molar concentrations. When one substitutes on a Ni^{2+} site a trivalent cation, such as Al^{3+}, this defect has an effective single positive charge ($Al^{\bullet}_{Ni}$). In a dilute solid solution (NiO-AlO□), this impurity then influences the concentration of defects through the electroneutrality condition:

$$[h^{\circ}] + [Al^{\bullet}_{Ni}] = □[V^{□'}], \quad (2)$$

with, in the extrinsic range:

$$[Al^{\bullet}_{Ni}] \approx \alpha[V^{\alpha'}], \quad (3)$$

and the nickel diffusion coefficient (D_{Ni}) (Philibert,1991) :

$$x_V D_V = x_{Ni} D_{Ni} \approx D_{Ni}, \quad (4)$$

where D_V is the vacancy diffusion coefficient, x_V the cationic vacancy concentration and x_i the mole fraction of Ni^{2+}, with $x_i=[Ni^{2+}]\approx 1$.

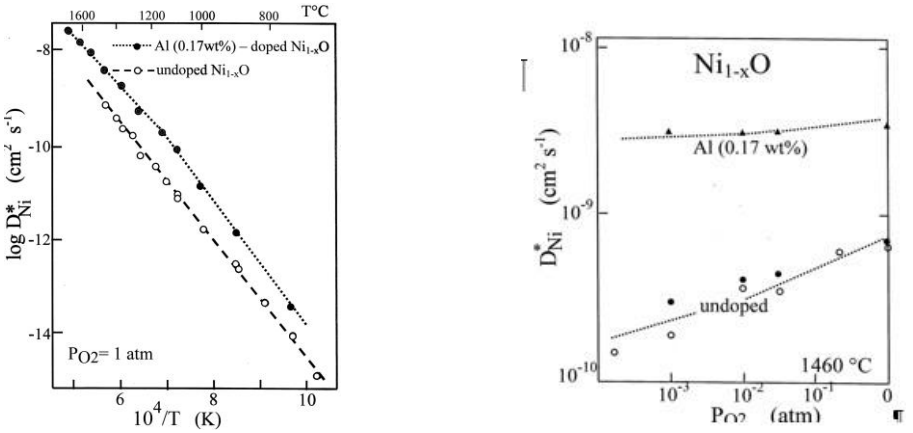

Figure 1. (a) Arrhenius plot of the self-diffusion coefficient of Ni^{2+} in undoped and Al-doped $Ni_{1-x}O$ single crystals and (b) oxygen partial pressure dependence of $D^*_{Ni,}$ at 1460°C.

Atkinson et al. (Atkinson,1981) have measured the self-diffusion of nickel (D^*_{Ni}) in undoped and Al (0.17wt%)-doped $Ni_{1-}xO$ single crystals between 700° and 1700°C, at an oxygen partial pressure P_{O2}=1atm. Their results reported in Fig.1 show that :

$$(D^*_{Ni})_{doped} > (D^*_{Ni})_{undoped} \quad (5)$$

Since the self-diffusion coefficient can be written (Philibert,1991).

$$D^*_{Ni} = f\, x_V D_V \quad (6)$$

where f is the correlation factor, the results reported in figure 1 are due to an increase of the cationic vacancy concentration (Eq.2).

Furthermore, a break is observed at T≈1200°C. In the lower temperature region (T<1200°C), the data are controlled by Al^{+3} (Eq.3). They are then obtained in the extrinsic range and indicate that the saturation solubility of Al in $Ni_{1-x}O$ is equal at 0.17 wt %.

Transport Proceses in a P-Type Semiconducting Oxide under Non-Equilibrium Conditions

One can recall that in cation deficient p-type semiconducting oxide solid solutions, the diffusivity of anions is much less than that of cations (Philibert,1991). One may then use the anion sublattice as frame of reference for motion of cations and defects. When an oxide (AO-BO□) is exposed to an oxygen chemical potential gradient (Eq.1), a flux of vacancies (J_V) occurs in the sample toward the side showing a low oxygen activity ($a_O = P_{O2}^{1/2}$), coupled to an opposite flux of cations (J_i) (Petot-Ervas, 1990; Halem, 2016; Philibert, 1972; Farhi, 1978; Atkinson, 1981; Mahiouz, 2019; Schmalzried, 1981, 1986).

$$J_V = -(J_A^{2+} + J_B^{\delta+}) \quad (7)$$

New lattice sites are then formed at the surface where cations arrive. The shift velocity of this surface and more generally the shift velocity of the oxidation front in the oxide, is given by(Petot-Ervas, 1990), (Halem, 2016), (Schmalzried, 1981):

$$v_{oxid} = J_V / C_M = -\Sigma J_i / C_M = -(J_A^{2+} + J_B^{\delta+})/C_M \quad (8)$$

If one neglects the correlation effects, it was shown (Petot-Ervas, 1990; Halem, 2016) that in a solid solution (AO-BOγ) under non-equilibrium conditions the flux of cations A and B can be written, with respect to the oxygen sublattice:

$$J_i = C_M D_i \left[-\frac{dx_i}{dz} + x_i\, \gamma\, \mathcal{F}\right] \quad (9)$$

where x_i is the local concentration of cations "i" in the cationic sublattice and ($\mathcal{F} = d\ln a_O/dz$) the driving force of diffusion, with according to Eq.1:

$$\mathcal{F} = d\ln a_O/dz = (1+\alpha)d\ln[V^{\alpha'}]/dz \quad (10)$$

Therefore, substituting Eq.10 in Eq.8, allows to show that the shift velocity of the oxidation front in an oxide AO-BOγ exposed to an oxygen chemical potential gradient can be written Petot-Ervas, 1990), (Halem, 2016; (Mahiouz, 2019):

$$v_{oxid} = J_V/C_M = -(D_A - D_B)dm/dz - D_A\, \mathcal{F}_{dop}, \quad (11)$$

while the shift velocity of the oxidation front in AO is expressed by the following relation:

$$v_{oxid} = -J_A^{2+}/C_M = -D_A\, \mathcal{F}_{AO} \quad (12)$$

where $m = x_B$ is the mole fraction of solute cations (B^{3+}) in the cationic sublattice, F_{dop} the driving force of diffusion in doped AO and F_{NiO} in undoped AO. Consequently, Eq.11 shows that the effect of solute cations on the oxido-reduction of a p-type semiconducting oxide depends not only on the diffusion coefficient of the

cations, as it was generally assumed until now (Kofstad , 1988), but also on the kinetic demixing of cations (dm/dz).

Results and Discussion

Experimental results in undoped and Al-doped $Ni_{1-x}O$ single crystals in non-equilibrium conditions

Cation Kinetic Demixing

This study was performed with undoped and Al (0.11 wt%)-doped $Ni_{1-x}O$ single crystals, machined to obtain parallelepipedic samples ($3x2x2mm^3$). Since the diffusing species are electrically charged, their fluxes may then be due to a gradient of oxygen activity (a_O), with $a_O=P_{O2}^{1/2}$ (Eq.10), or to an applied electric field (E) (Halem, 2016), (Mahiouz, 2019), (Monceau,1994):

$$F = q_iE/RT \quad (13)$$

where q_i is the charge of the diffusing species. From a practical point of view, it is easier to perform experiments in presence of an electrical field (experimental arrangement represented in the next section). A flux of cations occurs towards the cathode, where the cristal is reconstructed (Fig.2b), while an opposite flux of vacancies occurs in direction of the anode (Eq.7), which acts as a sink for these defects. Therefore, this leads to a shift of the sample end surfaces in direction of the cathode (Eqs.11,12).

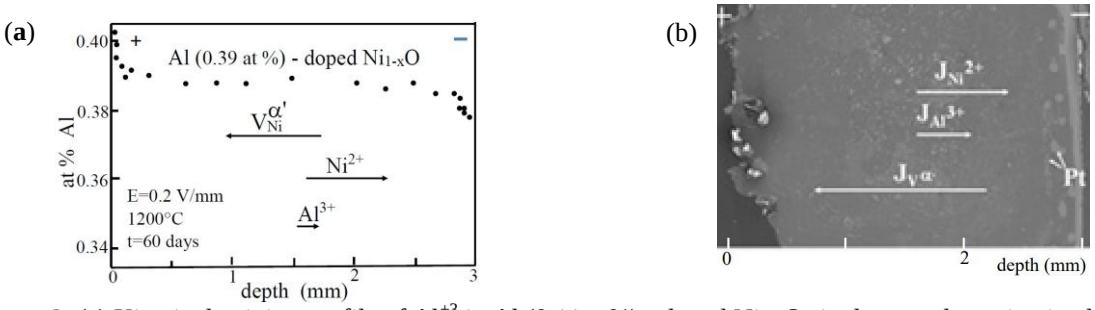

Figure 2. (a) Kinetic demixing profile of Al^{+3} in Al (0.11wt%) - doped $Ni_{1-x}O$ single crystals, maintained under 0.2V/mm, for 60 days, in air at 1200°C, and (b) cross section at the end of the experiment.

The results reported in figure 2 have been obtained with a parallelepipedic single crystal, of 3mm long. EPMA analyses on a polished cross-section at the end of experiments show an enrichment of Al^{+3} near the anode.

Therefore, it follows from Eq.9:

$$D_{Al}<D_{Ni} \quad (14)$$

Experimental Results in the Stability Range of $Ni_{1-x}O$ - Chemical Diffusion Coefficient

Experiments

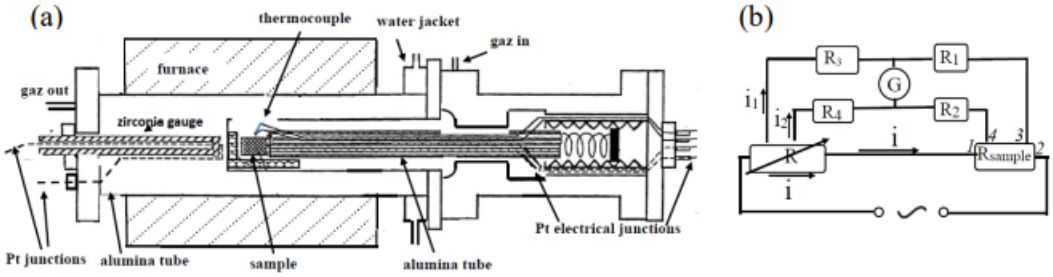

Figure 3. (a) Experimental arrangement for measuring electrical conductivity and (b) schematic representation of the Kelvin bridge.

The experimental arrangement is shown in figure 3. The measurements were performed from electrical conductivity measurements, by the four probe method at 1.5kHz frequency, using a Kelvin bridge (Fig.3b) whose equilibrium was checked by a fast detection amplifier (G). A thin layer of platinum was applied to the lower surfaces of the parallelepipedic sample (3x2x2 mm^3) connected to the voltage source (Fig.3b). The oxygen partial pressure was measured near the sample with an yttria stabized zirconia gauge (Fig.3b). Platinum wires (Pt) were used as electrical junctions (Halem, 2016).

Experimental Results

The results have been obtained with a single crystal, initially in equilibrium with the surrounding atmosphere (argon / $P_{O2}=10^{-3}$atm), by following the electrical conductivity as a function of time after a sudden change of P_{O2} (P_{O2}=0.21atm). Just after this change, the defect concentrations correspond to the new imposed condition at the solid-gas interface (Eq.1). A concentration gradient of cationic vacancies (dc_v/dz) sets up immediately near the surfaces (Eq.1), leading to a flux of these defects coupled to an opposite flux of cations (Eq.7) These fluxes progress in the bulk, pass through a maximum and decrease, until the new thermodynamical is reached. According to the Fick law, the coupled fluxes of cations (J_i) and cationic vacancies (J_V) can be written (Philibert,1991; (Kofstad, 1972; Farhi, 1978):

$$J_V=-\Sigma J_i=-\tilde{D}\ (dx_V/dz) \qquad (15)$$

where $\tilde{D}$ is the chemical diffusion coefficient

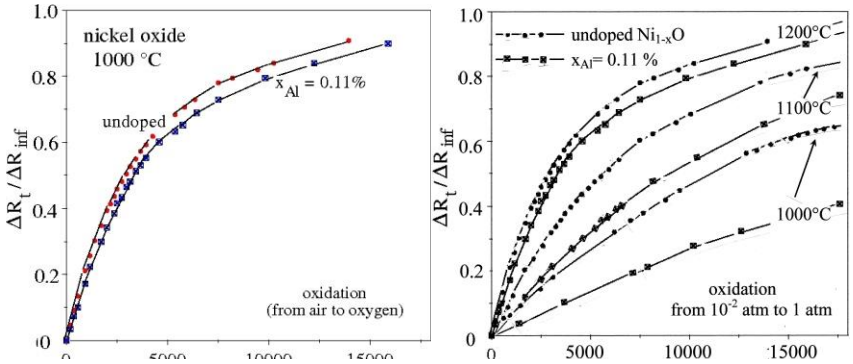

Figure 4. Re-equilibration kinetic of undoped and Al-doped $Ni_{1-x}O$ single crystals after an abrupt change of P_{O2}, followed by electrical conductivity measurements.

The results are reported in figure 4. They show that aluminium leads to a decrease of the oxidation rate. They are then in agreement with Eq.11. Indeed, after the change of P_{O2}, a kinetic demixing of cations occurs in the oxide. This leads to an enrichment of Al^{3+} in the side of the sample with a low concentration of cationic vacancies (Fig 2), i.e. near the surface exposed to a low P_{O2} (Eq.1) The two terms of Eq.11 have then opposite signs, leading to a decrease of v_{oxid}. Therefore, the agreement of Eq.11 with our results (Fig.4) shows that the kinetic demixing have a market influence on the oxydation rates of a p-type multi-component oxide.

On the other hand, the general relation of the electrical conductivity as a function of time ($\sigma(t)$) follows an exponential law. When the time increases, i.e. when the sample starts to reach its equilibrium condition, it was demonstrated that only the first term of this relation subsists (Farhi, 1978):

$$\frac{\sigma(t)-\sigma_\infty}{\sigma_0-\sigma_\infty}=\left(\frac{8}{\pi^2}\right)^3 \exp\left[-\pi^2\left(\frac{1}{H^2}+\frac{1}{L^2}+\frac{1}{l^2}\right)\tilde{D}t\right] \qquad (16)$$

where *H*, *L*, *l* are the sample dimensions, σ_0 the electrical conductivity before the equilibrium conditions are changed (t=0) and σ_∞ the conductivity when the new equilibrium is reached.

The chemical diffusion coefficient was then determined from the last linear part of the representations]:

$$\log(\sigma(t)-\sigma_{\infty}) = f(t)\,. \tag{17}$$

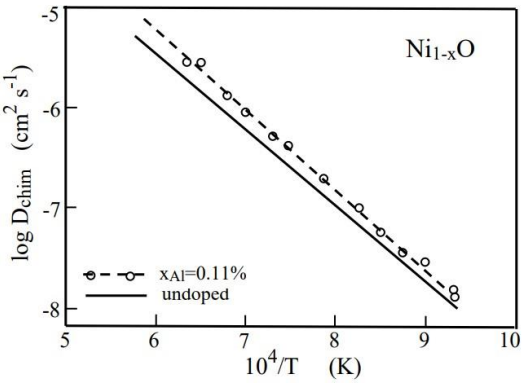

Figure 5. Influence of Al^{3+} on the chemical diffusion coefficient of $Ni_{1-x}O$. Comparaison with the values obtained with undoped $Ni_{1-x}O$.

The results obtained with the doped single crystal are reported in figure 5, together with the data determined for undoped $Ni_{1-x}O$ [15]. They show that Al^{3+} increases the oxidation kinetic of $Ni_{1-x}O$. Furthermore, these representations have the form of an Arrhenius equation (D=Do.exp(-□H/kT) (Philibert, 1972), which means that only one diffusion mechanism is dominant, as confirmed by the following results. Indeed, taking into account that the kinetic demixing processes are negligible in the last part of the representations $\log(\sigma(t)-\sigma_{\infty}) = f(t)$, it was shown that the chemical diffusion coefficient of undoped and Al-doped $Ni_{1-x}O$ single crystals can be expressed by the relation (Mahiouz, 2019) :

$$\tilde{D} \approx (1+\alpha)D_V \tag{18}$$

where D_V is the diffusion coefficient of the cationic vacancies ($V_M^{\alpha'}$) and □ their mean charge.

Furthermore, since the mean charge of the cationic vacancies does not change significantly for doped and undoped single crystals at higher P_{O2} ($P_{O2} \geq 10^{-2}$atm, □≈1.17±0.03 at 1000°C), it follows:

$$D_V(\text{Al-doped NiO}) > D_V(\text{undoped NiO}) \tag{19}$$

In addition, these results show that the increase of the diffusion coefficient of Ni^{2+} (Eq.6) observed in Al-doped $Ni_{1-x}O$ (Fig.1), explained previously by an increase of the concentration of cationic vacancies (Eq.2), is also due to an increase of the diffusion coefficient of the cationic vacancies (Eq.19).

Influence of Al on Nickel Oxidation

Experimental Results

The metal specimens were sintered from high purity Johnnson Mattey powders (Ni/99.99%, Al/99.50%), isostatically pressed at 1000bar, and sintered at 1100°C during 3h, under an Ar/H_2 atmosphere) (Halem, 2016). The obtained samples were then oxidized at 1250°C, during 30h. The oxide scale was removed on one main surface ($1cm^2$). This face was then slightly polished to a 1□m diamond finish. The experiments were performed in a Setaram thermobalance.

The results reported in figure 6 show the oxidation rate for pure and Ni-Al (0.5 wt %) polycrystalline coupons ($1cm^2$ by 0.1cm thick) from 700° to 1200°C, under P_{O2}=1atm. X-Ray analyses indicate that the scale developed on the samples were $Ni_{1-x}O$. Furthermore, in agreement with the Wagner theory Wagner, 1951),(Kofstad , 1988) , the results follow a parabolic law. The diffusion processes through the oxidation layer are then rate determining and the weight gain per unit area (Δm/s) can be expressed by Wagner (1951) and Kofstad (1988)

$$(\Delta m/s) = k_p \sqrt{t} + k_s \quad (20)$$

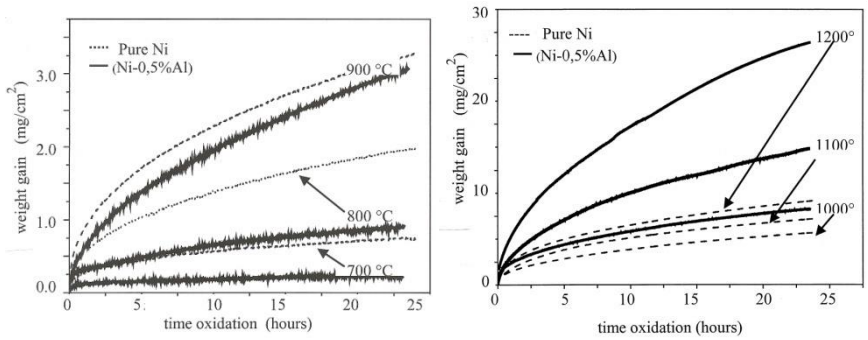

Figure 6. Isothermal weight gain versus time for Ni and Ni-(0.5%) Al alloy, under PO2=1atm

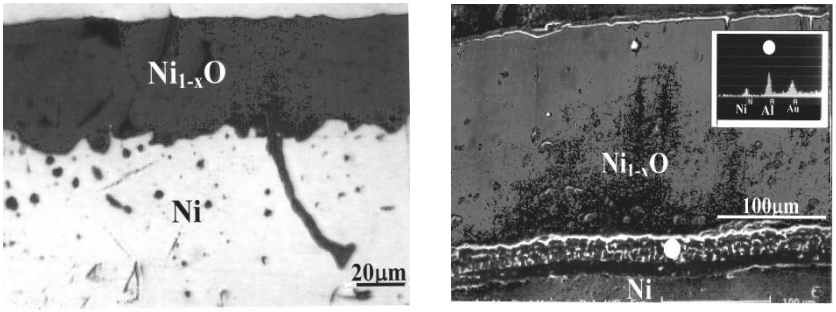

a) b)

Figure 7. Cross-sections (a) of Ni and (b) of Ni-(0.5%) Al after oxidation at 1200°C and EDAX analysis in the inner alloy oxidation layer.

At T<1000°C, the presence of Al leads (Fig.6) to a decrease of the oxidation rates in agreement with both, the results obtained with undoped and Al-doped $Ni_{1-x}O$ single crystals (Fig.4) and those obtained by Stott and Wood with Ni-(0.5 to 4 wt%) Al alloys (Stott,1977). Furthermore, cross section observations (Fig.7a) highlight an irregular nickel/oxide interface and an internal oxidation which pins the scale to the substrate.

At higher temperatures, it was found that the Ni-Al alloy oxidises faster than nickel and the oxide layer shows a duplex structure (Fig.7b), with columnar outer grains whose size increases with temperature. EDAX analyses reveal an enrichment of Al in the inner layer (Fig.7b). These results are in agreement with those obtained by Stott and Wood (Stott,1977). It should be noted that they are also in agreement with both, SIMS analyses (Atkinson, 1989) performed in layer grown on a Ni-(0.1 wt%) Cr alloy and EPMA profiles in layer grown on a Ni-(20%) Cr alloy (Atkinson, 1989), which also show an increase concentration of Cr in the inner oxidation scale. Furthermore, optical microscopy observations show that the oxidation scale on the Ni-Al alloy was not convoluted at all and did not really adhere to the metal, as was also observed by Stott et al (Stott,1977) and by Atkinson et al (Atkinson, 1989).

Discussion

In the present work, we have shown that the Ni-Al alloy oxidises more slowly than nickel, at T<1000°C, in agreement with the results obtained in the stability range of undoped and Al-doped $Ni_{1-x}O$ single crystals. The alloy oxidation kinetic is then governed by transport processes in the oxidation layer, i.e by the kinetic demixing of cations (Eq.9), which leads to both, a lower concentration of aluminium (Eq.12) and a decrease of D_{Ni} (Fig.2, Eq.5) in the outer oxidation scale.

At T≥1000°C, the oxidation scale grows faster than on high-purity Ni. One can recall both, that bulk diffusion in the oxide scale is dominant at high temperature and that oxygen grain boundary diffusion is too low to account for the observed influence of Al^{+3} (Kofstad, 1972). We have then considered a much faster transport mechanism than diffusion, such as the transport of oxygen molecules along fissures formed within the oxide, as suggested by Atkinson et al (1989, 1983). One can recall that these authors have investigated the mobility of oxygen during the growth of oxidation layers on high purity Ni and on dilute Ni-Cr alloys, whose properties of the

oxidation layers are closes to those on Ni-Al alloys (Halem, 2016). From sequential tracer oxidation experiments ($^{16}O_2$ and $^{18}O_2$) and secondary ion mass spectrometry (SIMS) analyses, they have found a large ^{18}O peak in the inner oxidation layer, showing an extensive penetration of the scale by the oxygen isotope, involving the transport of O_2 molecules along open channels, likely generated by compressive stresses attributed to NiO precipitates observed at room temperature in grain boundaries. We have confirmed this assumption taking into account the results obtained with both, undoped and doped $Ni_{1-x}O$ single crystals and oxidation scales grown on Ni-Al alloys. Indeed, it was shown both, that diffusivity of Ni^{2+} in $Ni_{1-x}O$ decreases with the amount of Al^{3+} (Fig.1, Eq.5) and that cation kinetic demixing processes occur in the growing oxidation scale (Fig.7b), leading to a lower concentration of Al^{3+} in the outer layer. Consequently, this depletion of Al^{3+} leads to a blocking effect on the diffusion of Ni^{2+} in the outer oxidation layer (Fig.7), causing a local excess of Ni. This promotes the formation of new oxide units in grain boundaries, leading to compressive stresses and the formation of fissures, whereby oxygen gas penetrates within the scale. It follows an increase concentration of cationic vacancies within the scale and an higher flux of these defects arriving at the metal/oxide interface, leading to an higher outward diffusion of Ni^{2+} responsible to an increase of the oxidation rate.

On the other hand, cross sections of oxidized samples (Fig 7) show different interface morphologies. These changes can be explained by an increase of the alloy oxidation rate. Indeed, the higher arrival of cationic vacancy at the metal/oxide interface prevents the metal/oxide interface to accommodate easily these defects, improving the formation of voids. In addition, a compressive stress appears at the interface due to the volume increase of the oxidation layer. These two coupled effects may then cause a low adherence at the metal/oxide interface, leading to a breakaway during cooling (Fig.7b).

Conclusion

In this work, we have analysed the thermal oxidation of Ni and of Ni-Al alloys, taking into account the thermodynamic and transport properties of undoped and Al-doped $Ni_{1-x}O$, single crystals. At T<1000°C, it was shown that the dilute Ni-Al alloy oxidises slower than nickel, in agreement with oxidation results obtained in the stability range of undoped and Al-doped $Ni_{1-x}O$ single crystals. A formal treatment has allowed us to show that the beneficial effect of Al can be explained by cation kinetic demixing processes in the oxidation layer, leading to both, a lower concentration of Al and a decrease of D_{Ni} in the outer layer. At higher temperatures, the oxidation scale grows faster on Ni-Al alloys than on high purity nickel. The transport of oxygen molecules along fissures was then suggested to explain these results. According to an ealier work performed with Ni-Cr alloys, we have assumed that their formation can be induced by compressive stresses in the growing oxide layer, generated by the formation of oxide units in grain boundaries observed at room temperature. The formation of these oxide units are due to both, the lower values of the diffusion coefficient of nickel when the concentration of Al^{+3} decreases and the depletion of Al^{+3} in the outer oxidation scale, resulting from cation kinetic demixing processes in the growing oxide layer. These oxide units generate compressive stresses and the formation of open channels whereby oxygen gas penetrates within the scale, leading to a faster outward diffusion of Ni^{2+}, responsible to a higher alloy oxidation rates. Furthermore, the penetration of oxygen in the scale also allows to explain the alloy/oxide interphase morphology, which does not adhere really and show a breakaway after cooling.

Scientific Ethics Declaration

The authors declare that the scientific ethical and legal responsibility of this article published in EPSTEM journal belongs to the authors.

Acknowledgements or Notes

* This article was presented as a poster presentation at the International Conference on Basic Sciences and Technology (www.icbast.net) held in Antalya/Turkey on November 16-19, 2023.

References

Atkinson, A. (1983). *Corrosion mass transport in solids* (p.97). M. Benniere & A. Catlow Eds., Plenum Press.

Atkinson, A., Hugues, A.E., & Hammou, A. (1981). The self diffusion of Ni in undoped and Al-doped NiO single crystals, *Philosophical Magazine A, 43(5),* 1071-1091.

Atkinson, A., & Smart, D .W. (1989). Transport of nickel and oxygen during the oxidation of nickel and dilute nickel/chromium alloys. *Journal of Elec. Chem. Society, 135*, 2886-2893.

Ben Abderrazik, G. (1986). *Mécanismes de croissance d'oxydes sur les alliages Fe-Cr-Al et Ni-Cr*. (Doctoral dissertation).Université Paris XI .

Catlow, A., & Mackrodt, W. (1986). *Non stoichiometric compounds, advances in ceramics* (4th ed., Volume 23). Defense Technical Information Center.

Farhi, R., & Petot-Ervas, G. (1978). Electrical conductivity and chemical diffusion coefficient measurements in single crystalline nickel oxide at high temperature. *Journal of Physical Chem. of Solids, 39*(11), 1169-1179.

Halem, Z., Halem, N., Abrudeanu, M., & Petot Ervas, G. (2016). Transport properties of Al or Cr–doped nickel oxide relevant to the thermal oxidation of diluted Ni-Al and Ni-Cr alloys. *Sol State Ionics, 297,* 13-18.

Kofstad, P. (1988) . *High temperature corrosion* (pp.382-385). Elsevier Applied Science.

Kofstad, P. (1972). *Diffusion and electrical conductivity in binary oxides*, Nonstoichiometry Wiley-Inter science

Kofstad, P., & Norby, T. (2007). *Defects and transport in crystalline solids* (pp.7-13). University of Oslo. Retrieved from https://www.uio.no

Mahiouz, H., Halem, Z., Halem, N., & Petot Ervas, G. (2019). Transport properties of Ce-doped nickel oxide and relevance to the oxidation of CeO_2-coated-nickel, *Solid State Ionics, 339,* 114943.

Monceau, D., Petot, C., & Petot Ervas, G. (1991). Kinetic demixing profile calculation in oxide solid solutions under a chemical potential gradient. *Sol.St.Ionics, 45* , 231-235.

Monceau. D., Filal, M., Tebtoub., M, Petot , C., Petot Ervas, G. (1994) . kinetic demixing of ceramics in an electrical field. *Solid State Ionics, 73,* 221-225.

Petot-Ervas, G., & Petot, C. (1990). The influence of impurities segregation phenomena on the oxido-reduction kinetic of oxides. *Journal of Physical Chem. of Solids,51*(8), 901-906.

Philibert, J. (1991). *Atom movements, editions de physique.* Les Ulis, France.

Schmalzried, H. (1981). *Solid state reactions* (2nd ed.). Florida, Basel.

Schmalzried, H. (1986). Behavior of (semiconducting) oxide crystals in oxygen potential gradients. *Reactivity of Solids, 1,117*-137.

Schmalzried, H., &Laqua, W. (1981). Multicomponent oxides in oxygen potential gradients. *Oxidation of Metals, 15,* 339-353.

Simlowitch, G., & Stubican, V. (1984). Transport in nonstoichiometric compounds. *NATO ASI, series B, Physics, 129.*

Stott, F.H., & Wood, G.C. (1977). The mechanism of oxidation of dilute Ni-Al alloys at 800-1200°C. *Corrosion Science, 17,* 647-670.

Wagner, C. (1951). *Atom movements.* Cleveland: American Ceramic Society for Metals.

Wood, G.C., & Hodgkiess, T. (1966). Oxidation of dilute Ni, Cr alloys, at 700-1200°C. *Nature, 211,*1358-1361.

Author Information

Nacer Halem
University Mouloud Mammeri
Tizi Ouzou, Algeria
Contact e-mail: nacer.halem@ummto.dz

Zohra Halem
University of Bouira
Bouira, Algeria

Petot Ervas Georgette
Centrale Supelec
Paris, France

To cite this article:

Halem, N., Halem, Z., & Georgette P.E. (2023). Thermal oxidation kinetics of nickel and dilute (Ni- Al) alloys. *The Eurasia Proceedings of Science, Technology, Engineering & Mathematics (EPSTEM), 25,* 187-195.